

# First search for $2\varepsilon$ and $\varepsilon\beta^+$ processes in $^{168}\text{Yb}$

P. Belli<sup>a</sup>, R. Bernabei<sup>a,b,1</sup>, R.S. Boiko<sup>c,d</sup>, F. Cappella<sup>e</sup>,  
 V. Caracciolo<sup>f</sup>, R. Cerulli<sup>a</sup>, F.A. Danevich<sup>c</sup>, M.L. di Vacri<sup>f,g</sup>,  
 A. Incicchitti<sup>e,h</sup>, B.N. Kropivnyansky<sup>c</sup>, M. Laubenstein<sup>f</sup>, S. Nisi<sup>f</sup>,  
 D.V. Poda<sup>c,i</sup>, O.G. Polischuk<sup>c</sup>, V.I. Tretyak<sup>c</sup>

<sup>a</sup>*INFN sezione Roma “Tor Vergata”, I-00133 Rome, Italy*

<sup>b</sup>*Dipartimento di Fisica, Università di Roma “Tor Vergata”, I-00133 Rome, Italy*

<sup>c</sup>*Institute for Nuclear Research, 03028 Kyiv, Ukraine*

<sup>d</sup>*National University of Life and Environmental Sciences of Ukraine, 03041 Kyiv, Ukraine*

<sup>e</sup>*INFN sezione Roma, I-00185 Rome, Italy*

<sup>f</sup>*INFN, Laboratori Nazionali del Gran Sasso, I-67100 Assergi (AQ), Italy*

<sup>g</sup>*Pacific Northwest National Laboratory, 902 Battelle Blvd, 99354, Richland WA, US*

<sup>h</sup>*Dipartimento di Fisica, Università di Roma “La Sapienza”, I-00185 Rome, Italy*

<sup>i</sup>*CSNSM, Univ. Paris-Sud, CNRS/IN2P3, Université Paris-Saclay, 91405 Orsay, France*

## Abstract

The double-electron capture and the electron capture with positron emission in  $^{168}\text{Yb}$  have been investigated for the first time at the STELLA facility of the Gran Sasso underground laboratory (Italy) measuring 371 g of highly purified ytterbium oxide placed on the end-cap of a 465 cm<sup>3</sup> ultra-low-background high purity Germanium detector (HPGe). No gamma associated to double beta processes in  $^{168}\text{Yb}$  have been observed after 2074 h of data taking. This has allowed setting the half-life limits on the level of  $\lim T_{1/2} \sim 10^{14} - 10^{18}$  yr at 90% C.L. Particularly, a lower half-life limit on a possible resonant

---

<sup>1</sup>Corresponding author. *E-mail address:* rita.bernabei@roma2.infn.it (R. Bernabei).

neutrinoless double-electron capture in  $^{168}\text{Yb}$  to the  $(2)^-$  1403.7 keV excited state of  $^{168}\text{Er}$  is set as  $T_{1/2} \geq 1.9 \times 10^{18}$  yr at 90% C.L. Half-life limits  $T_{1/2}^{2\nu(0\nu)} \geq 4.5(4.3) \times 10^{16}$  yr were set on the  $2\nu(0\nu)2\beta^-$  decay of  $^{176}\text{Yb}$  to the  $2^+$  84.3 keV first excited level of  $^{176}\text{Hf}$ .

*Keywords:* Double beta decay;  $^{168}\text{Yb}$ ;  $^{176}\text{Yb}$ ; Low counting gamma spectrometry; Purification of ytterbium

## 1 INTRODUCTION

Double beta ( $2\beta$ ) decays are rare processes of spontaneous nuclear disintegration which changes the charge of nuclei by two units. Double-electron capture ( $2\varepsilon$ ), electron capture with positron emission ( $\varepsilon\beta^+$ ) and double-positron decay ( $2\beta^+$ ) result in the charge decreasing, while double-electron decay ( $2\beta^-$ ) leads to charge increasing. Such processes are energetically allowed for 69 isotopes [1] among 286 naturally occurring primordial nuclides. Only 22 and 6 nuclides from the full list of 34 potentially  $2\varepsilon$ -active isotopes can also undergo  $\varepsilon\beta^+$  and  $2\beta^+$  decays, respectively. Being second order processes in the weak interaction, double beta decays are characterized by extremely long half-lives,  $\sim 10^{19}$  yr in the most favorable cases.

The main modes of  $2\beta$  processes are two-neutrino ( $2\nu$ ) double beta decay, in which two (anti)neutrinos are also appearing in the final state, and neutrinoless ( $0\nu$ )  $2\beta$  decay. The  $2\nu 2\beta$  decay is a Standard Model (SM) process, already observed in several nuclei with half-lives  $T_{1/2}^{2\nu 2\beta} \sim 10^{19} - 10^{24}$  yr [2, 3]. The  $0\nu 2\beta$  decay requires lepton number violation and a Majorana nature of neutrino, therefore, it is a unique tool to probe physics beyond the SM (for more details see recent reviews [4, 5, 6] and references therein). The current most stringent half-life limits on  $0\nu 2\beta^-$  decay are at the level of  $\lim T_{1/2}^{0\nu 2\beta} \sim 10^{24} - 10^{26}$  yr [3].

It should be emphasized that the above mentioned results are obtained in  $2\beta^-$  experiments, while the achievements in investigations of  $2\varepsilon/\varepsilon\beta^+/2\beta^+$  decays are much more modest. Indeed, there are only claims on the detection of the double-electron capture in  $^{130}\text{Ba}$  (there is a strong disagreement among the results of geochemical measurements, summarized in [2]) and  $^{78}\text{Kr}$  [7]. Moreover, the best experimental sensitivity to the nuclear charge decreasing  $2\beta$  processes is at the level of  $\lim T_{1/2}^{2\varepsilon/\varepsilon\beta^+/2\beta^+} \sim 10^{21} - 10^{22}$  yr (we refer reader

to references 53–62 in Ref. [8]). The reasons for this are: (i) small phase space factors, i.e., suppressed decay probabilities (e.g., compare the calculations for  $2\beta^-$  [9] with the ones for  $2\varepsilon/\varepsilon\beta^+/2\beta^+$  processes [10]); (ii) mostly very low natural abundances, typically less than 1%, with few exceptions [1]; (iii) experimental issues in the observation of a signature of the most favorable process, i.e.,  $2\nu 2\varepsilon$  capture (difficulties in precisely and/or with high efficiency detection of the emitted X-rays). At the same time, the searches for  $2\varepsilon/\varepsilon\beta^+/2\beta^+$  processes are well-motivated by the following considerations: (i) the detection of the  $2\nu$  mode provides an important information for the nuclear spectrometry and the measurement of the nuclear matrix elements to be compared with theoretical calculations (see e.g. [2]); (ii) the observation of the  $0\nu$  mode (or a limit compatible to ones for the  $0\nu 2\beta^-$  decay) would allow us to scrutinize the possible contribution of the hypothetical right-handed currents to the mechanism of neutrinoless double beta decay [11, 12, 13]; (iii) the rate of neutrinoless double-electron capture could be much faster thanks to a resonant enhancement caused by a mass degeneracy between the initial and final states [14, 15, 16, 17]. All together demand the development of experimental methods to increase the current sensitivity to  $2\beta$  processes. The main goal of the present work is the investigation of double beta decay processes in the ytterbium isotopes.

Table 1: Potentially  $2\beta$  decay active isotopes of ytterbium.

| Double $\beta$ transition                     | Energy release (keV) | Isotopic abundance (%) [18] | Decay channel                      |
|---|----------------------|-----------------------------|------------------------------------|
| $^{168}\text{Yb} \rightarrow ^{168}\text{Er}$ | 1409.27(25) [19]     | 0.123(3)                    | $2\varepsilon, \varepsilon\beta^+$ |
| $^{176}\text{Yb} \rightarrow ^{176}\text{Hf}$ | 1085.0(15) [20]      | 12.995(83)                  | $2\beta^-$                         |

Ytterbium contains two potentially double beta active nuclides:  $^{168}\text{Yb}$  and  $^{176}\text{Yb}$  (see Table 1). Thanks to a reasonably high energy release ( $Q_{2\beta}$ ), the  $2\varepsilon$  capture and  $\varepsilon\beta^+$  decay to the ground and to the several excited states of the daughter nucleus are energetically allowed in  $^{168}\text{Yb}$ . A simplified scheme of the  $^{168}\text{Yb}$  double beta decay transitions is presented in Fig. 1. The theoretical predictions on the  $^{168}\text{Yb}$   $2\nu 2\varepsilon$  capture rate [23] suggest that the detection of the decay to the ground state could be feasible with an expected half-life of  $2 \times 10^{23}$  yr, while the transition to the first  $0^+$  excited state (1217.2 keV) is experimentally unreachable due to the extremely long

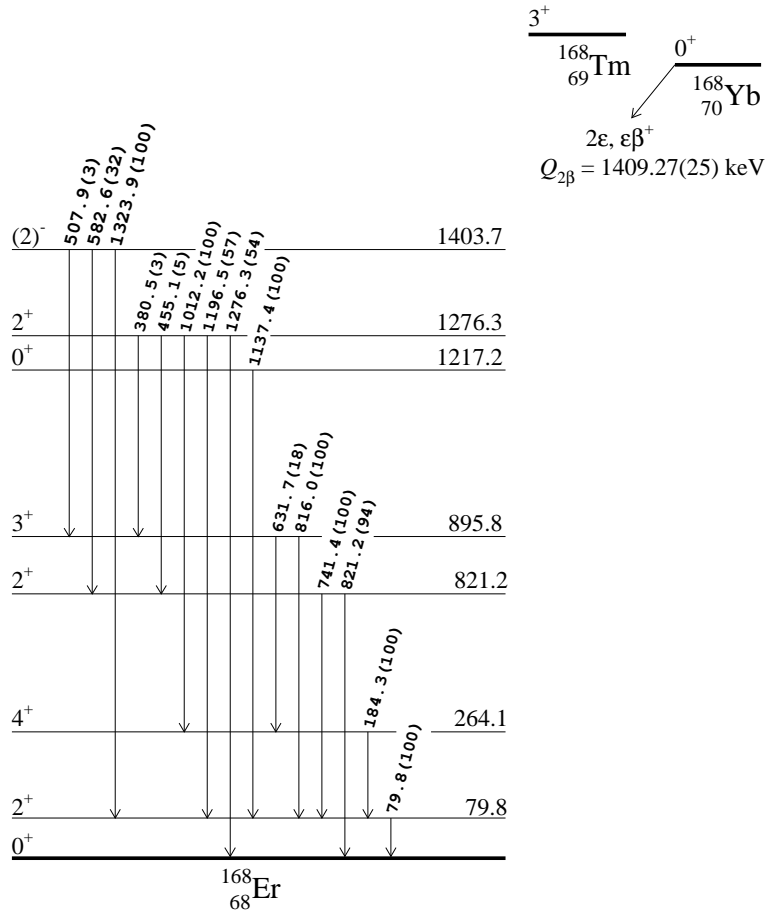


Figure 1: The simplified decay scheme of  $^{168}\text{Yb}$  [21]. The excited levels with spin 4 and higher are omitted, except the 264.1 keV level. The energies of the levels and of the emitted  $\gamma$  quanta are in keV. Only  $\gamma$  transitions with relative intensities of more than 2% are shown. The relative intensities of  $\gamma$  quanta are rounded to percent and given in parentheses.

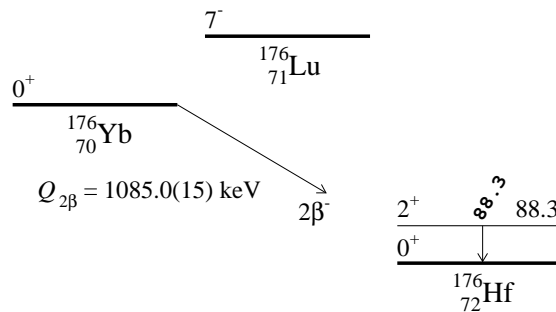


Figure 2: The simplified decay scheme of  $^{176}\text{Yb}$  [22]. The energies of the excited level and of the emitted  $\gamma$  quantum are given in keV.

expected half-life value of about  $10^{33}$  yr. Moreover, the isotope  $^{168}\text{Yb}$  was also proposed as a viable candidate for searches of resonant  $0\nu 2\varepsilon$  transitions [16, 24] and the expected half-lives are in the range of  $10^{23}$ – $10^{32}$  yr (assuming the value of the effective Majorana neutrino mass equal to 1 eV) [24]. The recent high precision measurements of the  $^{168}\text{Yb}$   $Q_{2\beta}$  value by the Penning-trap mass-ratio [19] restrict possible resonant transitions only to the 1403.7 keV excited level of  $^{168}\text{Er}$ . Up to now, no experimental results on  $^{168}\text{Yb}$  double beta decay half-lives were reported.

Another isotope of ytterbium,  $^{176}\text{Yb}$ , could reach via  $2\beta^-$  decay the ground and the first  $2^+$  excited level of  $^{176}\text{Hf}$  with energy 88.3 keV (see Fig. 2). Until now, only the  $2\beta^-$  transition to the 88.3 keV level was investigated and the achieved lower half-life limit was  $1.6 \times 10^{17}$  yr at 68% C.L. [25]. The isotope  $^{176}\text{Yb}$  is also promising for the neutrino detection [26] and the usage of a large-scale. Yb-containing detector for such purpose would open possibilities for high-sensitivity searches for  $2\beta$  processes in  $^{168}\text{Yb}$  and  $^{176}\text{Yb}$  [27]. It is also worth noting that an enrichment either in  $^{168}\text{Yb}$  or  $^{176}\text{Yb}$  to more than 15% and 97%, respectively (a factor of 120 and 7.5, respectively) was developed using a laser isotope separation technology [28].

The present work describes the searches for double beta decay in a sample of ytterbium oxide ( $\text{Yb}_2\text{O}_3$ ) using the ultra low background (ULB) gamma-ray spectrometry; therefore, only the  $2\beta$  processes resulting in the emission of X- and/or  $\gamma$ -rays could be detected with the used experimental technique. In addition, the work is also devoted to the study of the possibilities of ytterbium purification from radioactive elements, which is of particular interest for R&D of Yb-containing detectors of solar neutrinos and/or double beta decay.

## 2 Experiment

### 2.1 Purification of ytterbium oxide sample

A sample of  $\text{Yb}_2\text{O}_3$  powder ( $> 99.5\%$  TREO and  $> 99.999\%$  of  $\text{Yb}_2\text{O}_3/\text{TREO}$ ) has been purchased from Stanford Advanced Materials Corporation. The material contamination has been investigated by Inductively Coupled Plasma-Mass Spectrometry (ICP-MS, model Element II from Thermo Fisher Scientific, Waltham, Massachusetts, USA). The contaminants have been measured in Low Resolution (LR) mode, while Si, Cl, Ca, Cr and Fe were measured in Medium Resolution (MR) mode, and K was measured in High Resolution (HR) settings, respectively, to overcome isobaric interference issues. The results of the measurements are presented in Table 2, where the data of the material supplier are given too.

The radioactive contamination of the material has been studied using high-purity germanium (HPGe)  $\gamma$ -ray spectrometry at the STELLA (Sub-TERRanean Low Level Assay) facility of the Gran Sasso underground laboratory (Italy). A 340 h long measurement of a 627 g  $\text{Yb}_2\text{O}_3$  sample has been performed using a p-type detector, GePaolo (active volume of  $518 \text{ cm}^3$  and relative efficiency, with respect to a  $3'' \times 3''$  sodium iodine detector, of  $113\%$  [29]). The detection efficiencies to  $\gamma$  quanta in the full energy peak were simulated using the GEANT4 package [30, 31], and especially for the double beta decay processes by using the event generator DECAY0 [32, 33]. The intensities of the  $\gamma$  peaks in the energy spectra accumulated with and without the  $\text{Yb}_2\text{O}_3$  powder have been compared to estimate the activities (or upper limits on the activities) of the radioactive impurities. The activity of the  $^{228}\text{Ra}$  was estimated by analysis of the  $\gamma$  quanta emitted by its daughter  $^{228}\text{Ac}$ , the activity of  $^{228}\text{Th}$  was derived from  $^{212}\text{Pb}$ ,  $^{212}\text{Bi}$ , and  $^{208}\text{Tl}$ , the limit on  $^{226}\text{Ra}$  was obtained from analysis of  $^{214}\text{Pb}$  and  $^{214}\text{Bi}$ , the activities of  $^{235}\text{U}$ ,  $^{238}\text{U}$ ,  $^{234}\text{Th}$  and  $^{234m}\text{Pa}$  were found by analysis of the  $\gamma$  quanta expected in the decays of the nuclides. The HPGe measurements of the initial material (denoted in Tables 2 and 3 as “Before purification”) show traces of potassium ( $^{40}\text{K}$ ), lutetium ( $^{176}\text{Lu}$ ), radium ( $^{228}\text{Ra}$ ) and thorium ( $^{228}\text{Th}$ ). It should be stressed that the activities of  $^{40}\text{K}$ ,  $^{176}\text{Lu}$  and  $^{228}\text{Th}$  do contradict neither the data of the material supplier nor ICP-MS analysis of potassium, thorium and lutetium.

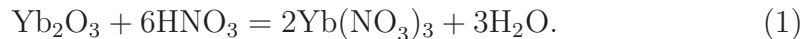
To reduce the observed radioactive contamination, purification of the material was performed using a combination of the sedimentation (precipitation)

Table 2: Concentration of impurities in the ytterbium oxide sample measured by ICP-MS before and after the purification. Uncertainties on the reported values are at the level of 30% (Semi-Quantitative mode of the ICP-MS measurements). Results of the ULB gamma-spectrometry measurements (see text and Table 3) are given in parentheses.

| Element | Concentration (ppm) |                     |                              |                    |
|---------|---------------------|---------------------|------------------------------|--------------------|
|         | Before purification |                     | Sediment after precipitation | After purification |
|         | Data of supplier    | Present measurement |                              |                    |
| Si      | 10                  | < 20                | -                            | -                  |
| Cl      | 50                  | -                   | -                            | -                  |
| K       | -                   | < 2 (0.8)           | 0.3                          | 0.3 (0.3)          |
| Ca      | 5                   | < 80                | -                            | -                  |
| Cr      | -                   | < 0.2               | -                            | -                  |
| Fe      | 1                   | 1.4                 | 1.8                          | 0.09               |
| Co      | -                   | 0.058               | -                            | -                  |
| Cu      | < 5                 | 0.6                 | -                            | -                  |
| Cs      | -                   | < 0.01              | -                            | -                  |
| La      | < 1                 | 0.01                | 0.002                        | 0.006 (< 0.15)     |
| Ce      | < 1                 | 0.05                | -                            | -                  |
| Eu      | < 1                 | < 1                 | -                            | -                  |
| Lu      | 1                   | - (7.6)             | < 15                         | < 15 (7.8)         |
| Pb      | -                   | 0.7                 | 0.3                          | 0.5                |
| Th      | -                   | 0.013 (0.019)       | 0.2                          | < 0.0005 (0.0003)  |
| U       | -                   | 0.0044 (< 0.012)    | 0.0014                       | 0.001 (< 0.001)    |

and liquid-liquid extraction [34] methods.

As a first step the ytterbium oxide sample was dissolved in a solution of  $\leq 67\%$  nitric acid (“HyperPur”, Alfa Aesar) in deionized water (18.2 M $\Omega$ -cm):



The analysis of the obtained solution has shown concentrations of 1.59 M for

Table 3: Radioactive contamination of the ytterbium oxide samples measured with ultra-low background HPGe  $\gamma$  detector with active volume of 518 cm<sup>3</sup> (627 g sample, before the purification) and in the course of the experiment with the help of HPGe  $\gamma$  detector with active volume of 465 cm<sup>3</sup> (371 g, after the purification). The uncertainties are given with  $\approx 68\%$  C.L., while the upper limits were evaluated with 90% C.L.

| Chain             | Nuclide            | Activity (mBq/kg)   |                    |
|-------------------|--------------------|---------------------|--------------------|
|                   |                    | Before purification | After purification |
|                   | <sup>40</sup> K    | 26 ± 9              | 9 ± 4              |
|                   | <sup>137</sup> Cs  | ≤ 1.8               | 1.1 ± 0.2          |
|                   | <sup>138</sup> La  | -                   | ≤ 0.12             |
|                   | <sup>152</sup> Eu  | -                   | ≤ 0.59             |
|                   | <sup>154</sup> Eu  | -                   | ≤ 0.24             |
|                   | <sup>176</sup> Lu  | 410 ± 30            | 420 ± 30           |
| <sup>232</sup> Th | <sup>228</sup> Ra  | 88 ± 5              | 2.6 ± 0.7          |
|                   | <sup>228</sup> Th  | 75 ± 4              | 1.1 ± 0.5          |
| <sup>235</sup> U  | <sup>235</sup> U   | ≤ 13                | ≤ 2.5              |
|                   | <sup>227</sup> Th  | -                   | ≤ 4.1              |
|                   | <sup>223</sup> Ra  | -                   | ≤ 4.6              |
|                   | <sup>211</sup> Pb  | -                   | ≤ 3.7              |
|                   | <sup>207</sup> Tl  | -                   | ≤ 34               |
| <sup>238</sup> U  | <sup>234</sup> Th  | ≤ 2100              | ≤ 240              |
|                   | <sup>234m</sup> Pa | ≤ 150               | ≤ 13               |
|                   | <sup>226</sup> Ra  | ≤ 2.8               | ≤ 0.83             |

Yb(NO<sub>3</sub>)<sub>3</sub> and of 0.9 M for the residual HNO<sub>3</sub>.

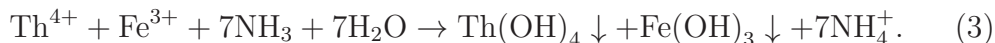
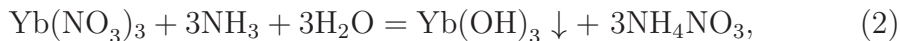
Then, the co-precipitation technique using fractional sedimentation of carrying ytterbium hydroxide Yb(OH)<sub>3</sub> was applied to remove low-soluble impurities from the solution, such as thorium and iron<sup>2</sup> hydroxides. Gaseous ammonia, produced from ammonium hydroxide solution (20.0%–30.0% NH<sub>3</sub> basis, ACS reagent, Sigma-Aldrich), was injected into the acidic solution (till pH = 6.5) to obtain ytterbium hydroxide which partially precipitated at this

---

<sup>2</sup>Purification of ytterbium oxide from iron (and other transition metals) was motivated by prospects of a future Yb-containing crystal scintillators development.



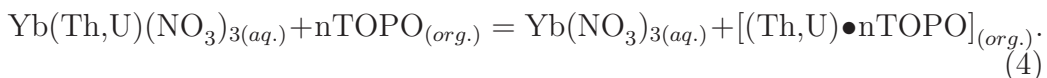
condition absorbing Th and Fe:



The obtained sediment (135 g, that is 21.6% of the initial amount of the material) was converted to  $\text{Yb}_2\text{O}_3$  form and analyzed by ICP-MS. The results of the measurement are presented in Table 2. The data show accumulation of Fe and especially of Th in the sediment, and therefore, confirm the ability of the sedimentation method to reduce contamination of the impurities in the initial  $\text{Yb}_2\text{O}_3$ .

The remaining aqueous solution of ytterbium nitrate was acidified to  $\text{pH} \sim 1$  and purified by the liquid-liquid extraction technique. The liquid-liquid extraction method has been proven to be the most effective technique for the purification of lanthanides from uranium and thorium traces [34, 35, 8]. A solution of 0.1 M tri-*n*-octylphosphine oxide (TOPO, 99%, Acros Organics) diluted in toluene ( $\leq 99.7\%$ , ACS reagent, Sigma-Aldrich) has been used as non-polar organic phase for the extraction of U and Th from the polar aqueous solution.

The two immiscible liquids were put into a separation funnel in volumetric ratio 1:1 and were shaken for several minutes. Uranium and thorium moved to the organic phase forming organometallic complexes by interaction with TOPO:



The purified aqueous solution was separated from the organic phase, and then ytterbium was precipitated from the solution in form of hydroxide by using ammonia gas. We expect that at this stage of the purification alkali and alkali-earth cationic impurities partially remained in the supernatant liquid. Finally, the obtained sediment was separated, dried and annealed at  $\approx 900^\circ\text{C}$  over several hours. As a result, 420 g of purified material have been obtained that is 67% of the initial material.

## 2.2 Measurements

A 371 g sample of the purified  $\text{Yb}_2\text{O}_3$  was placed in a cylindrical box of polystyrene (diameter 90 mm, height 50 mm) and placed on the end cap of the HPGe detector GeCris (active volume  $465 \text{ cm}^3$ , 120 % relative efficiency with respect to a  $3'' \times 3''$  sodium iodine detector) [29]) of the STELLA facility of the Gran Sasso underground laboratory. The  $\gamma$  spectrometer is shielded all around by  $\approx 25$  cm of low radioactive lead,  $\approx 5$  cm copper, and  $\approx 2.5$  cm Roman lead in the innermost part. The set-up is enclosed in an air-tight poly(methyl methacrylate) box and flushed with high purity nitrogen gas to reduce as much as possible the environmental radon concentration. The energy dependence of the detector resolution is described by the following function:  $\text{FWHM}(\text{keV}) = \sqrt{1.41 + 0.00197 \times E_\gamma}$ , where  $E_\gamma$  is in keV. The energy spectrum with the  $\text{Yb}_2\text{O}_3$  sample was gathered over 2074 h and the background spectrum was measured over 1046 h. The spectra normalized on time of measurements, are shown in Fig. 3.

There was still some excess in the  $\gamma$  peaks of  $^{40}\text{K}$ ,  $^{137}\text{Cs}$ ,  $^{176}\text{Lu}$ , and  $^{232}\text{Th}$  daughters in the data of the purified  $\text{Yb}_2\text{O}_3$  sample. The estimations of the radioactive contamination of the sample after purification are presented in Table 3. Unfortunately, the contamination in lutetium remained the same due to the high chemical affinity of ytterbium and lutetium, while the concentrations of potassium, radium and thorium was reduced by factors of 3, 34 and 68, respectively.

## 3 Searches for $2\beta$ processes in $^{168}\text{Yb}$ and $^{176}\text{Yb}$

The energy spectrum of the  $\text{Yb}_2\text{O}_3$  sample (see Fig. 3) does not contain peculiarities which could be ascribed to double beta decay processes in ytterbium isotopes. Therefore, the data have been analyzed estimating lower half-life limits for the  $2\varepsilon$  and the  $\varepsilon\beta^+$  decay of  $^{168}\text{Yb}$  and  $2\beta^-$  decay of  $^{176}\text{Yb}$  using the following formula:

$$\lim T_{1/2} = \ln 2 \cdot N \cdot t \cdot \eta / \lim S,$$

where  $N$  is the number of potentially  $2\beta$  active nuclei in the  $\text{Yb}_2\text{O}_3$  sample,  $t$  is the time of measurement,  $\eta$  is the detection efficiency for a considered  $2\beta$  channel, and  $\lim S$  is the upper limit on the number of events of the effect searched for, which can be excluded at a given confidence level (C.L.).

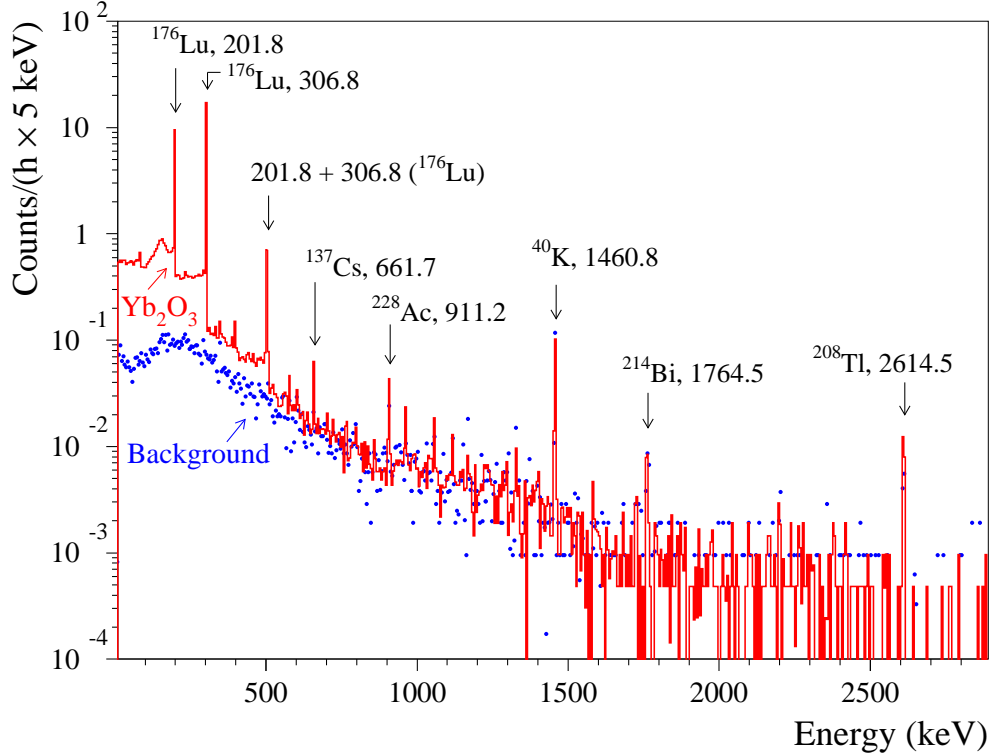


Figure 3: The energy spectra measured with the ULB HPGe  $\gamma$  spectrometer with the  $\text{Yb}_2\text{O}_3$  sample over 2074 h ( $\text{Yb}_2\text{O}_3$ ) and without the sample over 1046 h (Background). The energies of the most prominent  $\gamma$  peaks are given in keV.

The EGSnrc-based Monte Carlo simulations [36] with initial kinematics given by the DECAY0 event generator [32, 33] have been performed to calculate the detection efficiencies. The Monte Carlo simulations have been shown to be accurate by comparison with experimental data obtained with a  $^{133}\text{Ba}$   $\gamma$  calibration source. The areas of the  $^{133}\text{Ba}$   $\gamma$  peaks with energies 276 keV, 303 keV, 356 keV and 384 keV agree with the experimental data within 1%, while the low energy peak at 81 keV is smaller than the experimental one by 28%. The discrepancy for the low energy  $\gamma$  quanta can be explained by difficulties to reconstruct precisely the experimental geometry (in particular, the effect could be due to the source holder that caused some additional absorption of low energy  $\gamma$  quanta).

By fitting the data with the models accounting for the effect searched

for and for the background, the  $\lim S$  has been estimated according to the Feldman-Cousins recommendations [37]. All the  $\lim S$ , and thus the half-life limits in the present work, are given at 90% C.L. The contributions of systematic errors, e.g. uncertainties of the energy calibration and resolution, the number of  $2\beta$  active nuclei, and time of measurements are negligible in comparison to the statistical fluctuations of the excluded peak areas. Uncertainties of the Monte Carlo calculated detection efficiencies may have some merit at the energies less than  $\sim 270$  keV as it was demonstrated by the comparison of the Monte Carlo simulation and experimental data obtained with the  $^{133}\text{Ba}$  source. Nevertheless, we decided to include only statistical errors coming from the data fluctuations in the half-life limits estimations.

### 3.1 Double-electron capture in $^{168}\text{Yb}$

A cascade of X rays and Auger electrons with energies 47.7 – 57.5 keV is the expected signature of the  $2\nu 2K$  capture in  $^{168}\text{Yb}$  with the transition to the ground state of  $^{168}\text{Er}$ . In the analysis we considered the most intense X rays of erbium [38]:  $E_1 = 48.2$  keV (the intensity is  $I_1 = 27.0\%$ ),  $E_2 = 49.1$  keV ( $I_2 = 47.5\%$ ),  $E_3 = 55.5$  keV ( $I_3 = 5.1\%$ ),  $E_4 = 55.7$  keV ( $I_4 = 9.8\%$ ), and  $E_5 = 57.1$  keV ( $I_5 = 3.3\%$ ). The detection efficiency for  $\gamma$  quanta in the energy interval 49 – 57 keV was calculated using the EGSnrc-based Monte Carlo code. The detection efficiency at such a low energy strongly depends on energy and can be approximated in the energy interval 48 – 57 keV as following:  $\eta = 7.639 \times 10^{-3} - 3.151 \times 10^{-4} \times E + 3.260 \times 10^{-6} \times E^2$ , where  $E$  is in keV. The whole distribution of the expected X-ray peaks was built by accounting for the intensities  $I_i$  and the efficiencies at the energies  $E_i$ . Then, the energy spectrum of the  $\text{Yb}_2\text{O}_3$  sample, in the region of interest, was fitted with the sum of the five Gaussians (normalized to the total area equal 1) and a first-degree polynomial to model the continuous background (see Fig. 4). The best fit ( $\chi^2/\text{n.d.f.} = 55.6/62 = 0.864$ , where n.d.f. is number of degrees of freedom), in the energy interval (34 – 66) keV, gives  $(21.8 \pm 79.1)$  counts for the  $2\nu 2K$  effect. According to [37], the  $\lim S$  value was calculated to be 152 counts. The detection efficiency for the five peaks was calculated as  $\Sigma I_i \times \eta_i = 5.82 \times 10^{-5}$ , where  $\eta_i$  is the detection efficiency at energy  $E_i$ . Finally, considering that  $1.39 \times 10^{21}$  nuclei of  $^{168}\text{Yb}$  are in the  $\text{Yb}_2\text{O}_3$  sample, one obtains the following half-life limit for the  $2\nu 2K$  capture in  $^{168}\text{Yb}$ :  $T_{1/2} \geq 8.7 \times 10^{13}$  yr. The simulated efficiency at the 81 keV for  $^{133}\text{Ba}$  source was lower than the measured one, thus our  $T_{1/2}$  limit for the

$2\nu 2K$  process is rather conservative.

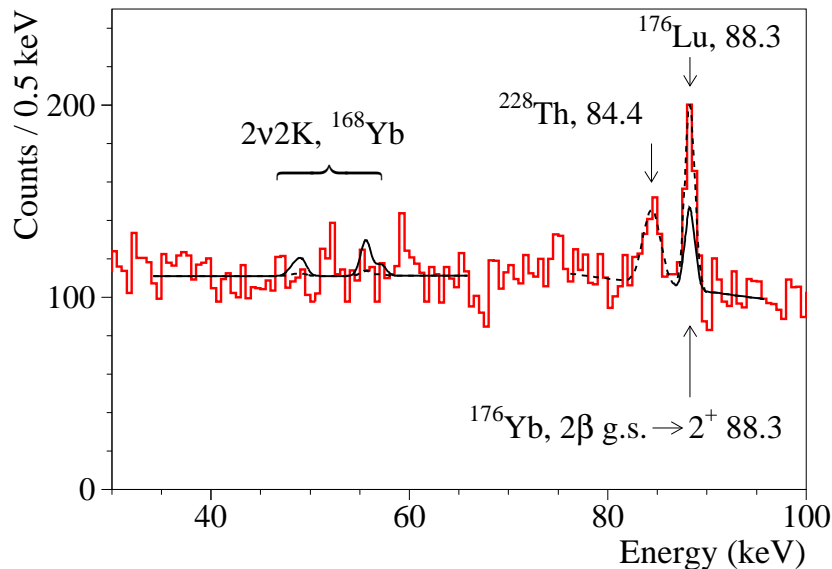


Figure 4: A low energy part of the spectrum accumulated by the ultra-low background  $\gamma$  spectrometer with the  $\text{Yb}_2\text{O}_3$  sample over 2074 h. The approximation function and the excluded effect of  $2\nu 2K$  capture in  $^{168}\text{Yb}$  are shown by dashed and solid lines, respectively. The fit of the data in the vicinity of the  $2\beta^-$  transition of  $^{176}\text{Yb}$  to the first excited level (88.3 keV) of  $^{176}\text{Hf}$  (dashed line) and the excluded peak of the effect (solid line) are also shown. The energies of the  $\gamma$  peaks are given in keV.

In case of  $2\nu 2\varepsilon$  decays of  $^{168}\text{Yb}$  to excited states of  $^{168}\text{Er}$ , only the transitions to  $0^+$  and  $2^+$  levels were considered. The spectrum with the  $\text{Yb}_2\text{O}_3$  sample has been fitted in the various energy intervals, where the most intense  $\gamma$  quanta are expected to be emitted in the de-excitation processes (see Fig. 1). The background models were built from a Gaussian function describing the effect (a peak with the energy of the considered de-excitation  $\gamma$  quanta), a continuous background and additional Gaussian(s) if it was also needed to approximate neighboring  $\gamma$  peak(s) coming from environmental radioactivity and/or internal contamination of the  $\text{Yb}_2\text{O}_3$ . The derived half-life limits are reported in Table 4.

In the searches for neutrinoless double-electron capture in  $^{168}\text{Yb}$  to the ground state of  $^{168}\text{Er}$ , we have considered only captures from  $K$  and/or  $L$

Table 4: Half-life limits on  $2\beta$  processes in  $^{168}\text{Yb}$  and  $^{176}\text{Yb}$ , established in the present work. All the limits are given with 90% C.L.

| Process of $2\beta$ decay                     | Decay mode | Level of daughter nucleus (keV) | Signature $E_\gamma$ (keV) | Detection efficiency   | lim $S$ (counts) | Half-life limit (yr)      |
|---|------------|---------------------------------|----------------------------|------------------------|------------------|---------------------------|
| $^{168}\text{Yb} \rightarrow ^{168}\text{Er}$ |            |                                 |                            |                        |                  |                           |
| $2K$  | $2\nu$     | g.s.                            | 48–57                      | $5.818 \times 10^{-5}$ | 152              | $\geq 8.7 \times 10^{13}$ |
| $2\varepsilon$                                | $2\nu$     | $2^+$ 79.8                      | 79.8                       | $3.974 \times 10^{-4}$ | 40               | $\geq 2.3 \times 10^{15}$ |
| $2\varepsilon$                                | $2\nu$     | $2^+$ 821.2                     | 821.2                      | $1.275 \times 10^{-2}$ | 6.6              | $\geq 4.4 \times 10^{17}$ |
| $2\varepsilon$                                | $2\nu$     | $0^+$ 1217.2                    | 1137.4                     | $2.311 \times 10^{-2}$ | 3.5              | $\geq 1.5 \times 10^{18}$ |
| $2\varepsilon$                                | $2\nu$     | $2^+$ 1276.3                    | 1276.3                     | $5.296 \times 10^{-3}$ | 1.4              | $\geq 8.6 \times 10^{17}$ |
| $2K$  | $0\nu$     | g.s.                            | 1294.0–1294.5              | $2.180 \times 10^{-2}$ | 6.8              | $\geq 7.3 \times 10^{17}$ |
| $KL$  | $0\nu$     | g.s.                            | 1341.8–1343.7              | $2.142 \times 10^{-2}$ | 7.1              | $\geq 6.9 \times 10^{17}$ |
| $2L$  | $0\nu$     | g.s.                            | 1389.5–1392.8              | $2.101 \times 10^{-2}$ | 3.9              | $\geq 1.2 \times 10^{18}$ |
| $2\varepsilon$                                | $0\nu$     | $2^+$ 79.8                      | 79.8                       | $7.698 \times 10^{-5}$ | 40               | $\geq 4.4 \times 10^{14}$ |
| $2\varepsilon$                                | $0\nu$     | $2^+$ 821.2                     | 821.2                      | $1.126 \times 10^{-2}$ | 6.6              | $\geq 3.9 \times 10^{17}$ |
| $2\varepsilon$                                | $0\nu$     | $0^+$ 1217.2                    | 1137.4                     | $2.310 \times 10^{-2}$ | 3.5              | $\geq 1.5 \times 10^{18}$ |
| $2\varepsilon$                                | $0\nu$     | $2^+$ 1276.3                    | 1276.30                    | $5.307 \times 10^{-3}$ | 1.4              | $\geq 8.6 \times 10^{17}$ |
| Resonant $M_1M_1$                             | $0\nu$     | $(2)^-$ 1403.7                  | 1323.9                     | $1.590 \times 10^{-2}$ | 1.9              | $\geq 1.9 \times 10^{18}$ |
| $\varepsilon\beta^+$                          | $2\nu$     | g.s.                            | 511                        | $6.277 \times 10^{-2}$ | 51               | $\geq 2.8 \times 10^{17}$ |
| $\varepsilon\beta^+$                          | $2\nu$     | $2^+$ 79.8                      | 511                        | $6.274 \times 10^{-2}$ | 51               | $\geq 2.8 \times 10^{17}$ |
| $\varepsilon\beta^+$                          | $0\nu$     | g.s.                            | 511                        | $6.190 \times 10^{-2}$ | 51               | $\geq 2.8 \times 10^{17}$ |
| $\varepsilon\beta^+$                          | $0\nu$     | $2^+$ 79.8                      | 511                        | $6.223 \times 10^{-2}$ | 51               | $\geq 2.8 \times 10^{17}$ |
| $^{176}\text{Yb} \rightarrow ^{176}\text{Hf}$ |            |                                 |                            |                        |                  |                           |
| $2\beta^-$                                    | $2\nu$     | $2^+$ 88.3                      | 88.3                       | $1.958 \times 10^{-4}$ | 106              | $\geq 4.5 \times 10^{16}$ |
| $2\beta^-$                                    | $0\nu$     | $2^+$ 88.3                      | 88.3                       | $1.907 \times 10^{-4}$ | 106              | $\geq 4.3 \times 10^{16}$ |

shells (as the most probable). It was also supposed that the energy excess in the process is taken away by (bremsstrahlung)  $\gamma$  quanta with an energy  $E_\gamma = Q_{2\beta} - E_{b1} - E_{b2}$ , where  $E_{b1}$  and  $E_{b2}$  are the binding energies of the captured electrons on the atomic shells of the daughter erbium atom. The energy spectrum measured with the  $\text{Yb}_2\text{O}_3$  sample was then fitted by a model constructed in the same way as in the above-mentioned analysis of the  $2\nu 2\varepsilon$  decays of  $^{168}\text{Yb}$  to the excited states of  $^{168}\text{Er}$ . However, the energy of the Gaussian function used to describe the effect was varied according to the uncertainty of the  $Q_{2\beta}$  value and, for the captures involving the  $L$  shells, to the difference between the binding energies of  $L_1$  and  $L_3$  shells. The fits to the energy spectrum find  $(3.2 \pm 2.2)$ ,  $(3.2 \pm 2.4)$ , and  $(1.6 \pm 1.4)$  counts for the  $0\nu 2K$ ,  $0\nu KL$ , and  $0\nu 2L$  peaks respectively and the corresponding  $\text{lim } S$  values are 6.8, 7.1 and 3.9 counts. The excluded peaks of the  $0\nu$  double-electron captures in  $^{168}\text{Yb}$  to the ground state of  $^{168}\text{Er}$  are shown in Fig. 5, while the obtained lower half-life limits on these  $2\beta$  processes are given in Table 4.

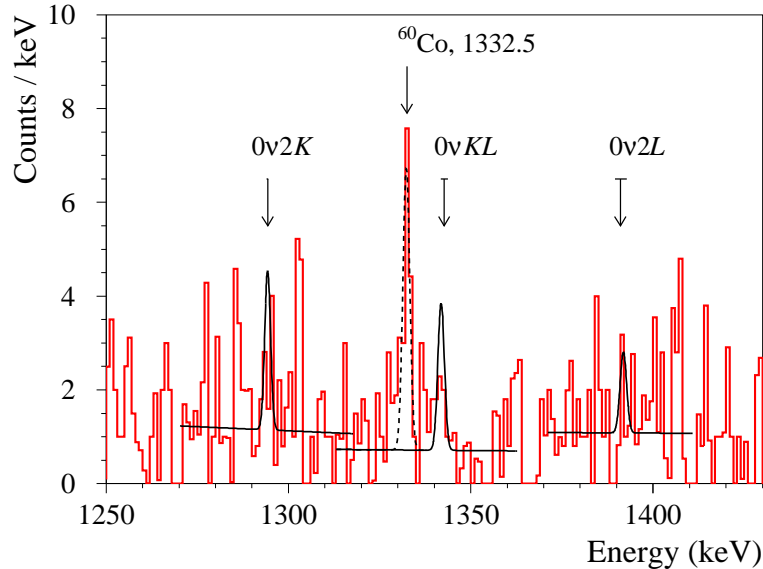


Figure 5: An interval of the energy spectrum accumulated with the  $\text{Yb}_2\text{O}_3$  sample over 2074 h, where the  $\gamma$  peaks from the  $0\nu 2K$ ,  $0\nu KL$ , and  $0\nu 2L$  captures in  $^{168}\text{Yb}$  to the ground state of  $^{168}\text{Er}$  are expected. The 90% C.L. excluded peaks are shown by solid lines. The fit of the background peak of  $^{60}\text{Co}$  with energy 1332.5 keV is shown by the dashed line.

The  $2\varepsilon$  decay of  $^{168}\text{Yb}$  is also allowed to excited levels of  $^{168}\text{Er}$ , however the  $0\nu$  and  $2\nu$  modes cannot be distinguished by  $\gamma$ -ray spectrometry. The detection efficiencies for  $0\nu$  and  $2\nu$  modes are slightly different due to emission of additional  $\gamma$  quanta in the  $0\nu 2\varepsilon$  decay with energy  $E_\gamma = Q_{2\beta} - E_{b1} - E_{b2} - E_{exc}$ , where  $E_{exc}$  is the energy of the excited level of  $^{168}\text{Er}$ . So, using the results of fits in the energy intervals where intense  $\gamma$  peaks are expected, we obtained limits on the  $0\nu 2\varepsilon$  decays of  $^{168}\text{Yb}$  to the  $0^+$  and  $2^+$  excited levels of  $^{168}\text{Er}$  (see Table 4).

The rate of the  $0\nu 2\varepsilon$  capture in  $^{168}\text{Yb}$  to the excited levels of  $^{168}\text{Er}$  could be resonantly enhanced thanks to the possible degeneracy of the energy release. Taking into account the recent precise measurements of the  $^{168}\text{Yb}$   $Q_{2\beta}$  value [19] and the nuclear structure of  $^{168}\text{Er}$  [21], the lowest degeneracy  $Q_{2\beta} - E_{b1} - E_{b2} - E_{exc} = 1.16$  keV can be achieved in the  $0\nu M_1 M_1$  decay of  $^{168}\text{Yb}$  to the  $(2)^-$  1403.7 keV level of  $^{168}\text{Er}$ . However, no substantial resonant enhancement of the decay probability is foreseen for the degeneracy on the 1-keV-level (e.g., see Fig. 10 in [39]). Moreover, the capture of two electrons from higher orbitals, as well as the transition between  $0^+$  and  $(2)^-$  states<sup>3</sup>, additionally suppress the probability of the decay. Nevertheless, we have performed the search for this process too and the absence of 1323.9 keV de-excitation  $\gamma$  quanta in the background spectrum of the  $\text{Yb}_2\text{O}_3$  sample was used to set a half-life limit  $T_{1/2} \geq 1.9 \times 10^{18}$  yr.

## 3.2 Electron capture with positron emission in $^{168}\text{Yb}$

We considered  $\varepsilon\beta^+$  decay of  $^{168}\text{Yb}$  with the transition to the ground and to the first  $2^+$  (79.8 keV) excited states of  $^{168}\text{Er}$ , taking into account the maximal kinetic energy available for the emitted positron (up to  $\approx 387$  keV, depending on the binding energy of the atomic shell of the daughter erbium atom). Irrespective to the  $2\nu$  and  $0\nu$  modes and/or the transition level, the highest detection efficiency in these processes is expected for a 511 keV  $\gamma$  peak, populated by two 511 keV  $\gamma$  quanta emitted in the positron-electron annihilation. The fits of the background spectra of the HPGe detector acquired with the  $\text{Yb}_2\text{O}_3$  powder and without sample (see Fig. 6) find the area of the annihilation peak  $(25 \pm 13)$  and  $(19 \pm 18)$  counts, respectively. We should add to the model a sum peak with energy  $(201.8 + 306.8)$  keV = 508.6

---

<sup>3</sup>Not precise knowledge of the  $^{168}\text{Er}$  nuclear structure leaves a possibility of more favorable ( $0^+ \rightarrow 0^-$ ) transition.



keV caused by the  $^{176}\text{Lu}$  internal contamination of the  $\text{Yb}_2\text{O}_3$  sample. Taking into account the time of measurements of the sample and of the background data,  $(-12 \pm 38)$  events can be ascribed to the extra rate of the 511 keV peak in the data accumulated with the ytterbium oxide sample, resulting in the  $\text{lim } S$  value equal to 51 counts. Taking into account the rather similar detection efficiencies for 511 keV  $\gamma$  quanta emitted in the  $\varepsilon\beta^+$  decay processes in  $^{168}\text{Yb}$ , we obtained for the both  $2\nu$  and  $0\nu$  modes of  $\varepsilon\beta^+$  decay the same half-life limit  $\text{lim } T_{1/2} = 2.8 \times 10^{17}$  yr.

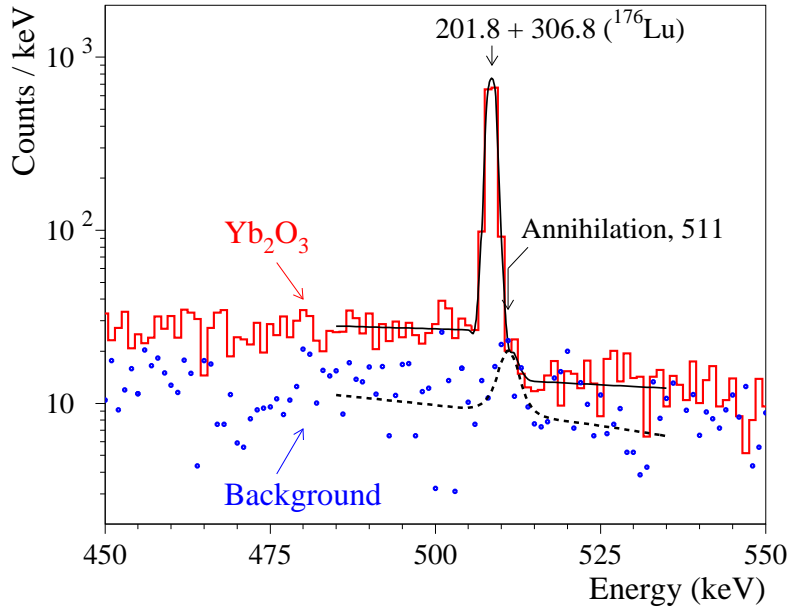


Figure 6: Parts of the energy spectra measured with the ytterbium oxide sample over 2074 h (histogram) and background over 1046 h (points) in the vicinity of the annihilation peak. The energies of the  $\gamma$  peaks are in keV.

### 3.3 $2\beta^-$ decay of $^{176}\text{Yb}$ to the first excited level of $^{176}\text{Hf}$

The double beta decay of  $^{176}\text{Yb}$  is energetically allowed to the ground and to the first  $2^+$  excited (88.3 keV) states of  $^{176}\text{Hf}$ , but only the transition to the excited level could be investigated in the present experiment. The energy spectrum measured with the  $\text{Yb}_2\text{O}_3$  sample was fitted in the energy interval 76 – 96 keV by a model built of two Gaussian functions to describe

the effect searched for and the background 84.4 keV  $\gamma$  peak of  $^{228}\text{Th}$ , and a first degree polynomial as a background model. The fit of the data (see Fig. 4) finds an area of the 88.3 keV peak of  $239 \pm 26$  counts. However, taking into account the contamination of the sample by  $^{176}\text{Lu}$ ,  $181 \pm 13$  counts should be ascribed to the  $^{176}\text{Lu}$  activity. The difference is  $58 \pm 29$  counts; although this difference is 2 sigma from zero, it cannot be interpreted as the effect searched for. Thus, the number of events excluded at 90% C.L. according to [37] is  $\lim S = 106$  counts. Taking into account the number of  $^{176}\text{Yb}$  nuclei in the sample ( $1.473 \times 10^{23}$ ) and the detection efficiency  $\eta^{2\nu} = 1.958 \times 10^{-4}$  ( $\eta^{0\nu} = 1.907 \times 10^{-4}$ ), we set the following half-life limits for the  $2\beta^-$  decay of  $^{176}\text{Yb}$  to the first  $2^+$  excited state of  $^{176}\text{Hf}$ :  $T_{1/2}^{2\nu(0\nu)} \geq 4.5(4.3) \times 10^{16}$  yr. The achieved limit is weaker than the one ( $T_{1/2}^{2\beta^-} \geq 1.6 \times 10^{17}$  yr at 68% C.L.) obtained in the experiment [25] with a similar technique for the sum of the  $2\nu$  and  $0\nu$  modes of the decay. The reason for the worse sensitivity of the present experiment is the contamination of the sample by lutetium.

## 4 CONCLUSIONS

The double beta decay processes in  $^{168}\text{Yb}$  have been investigated for the first time using a highly purified 371 g  $\text{Yb}_2\text{O}_3$  sample and a ultra-low-background  $465 \text{ cm}^3$  HPGe  $\gamma$  spectrometer. The experiment has been carried out at the STELLA facility of the Gran Sasso underground laboratory over 2074 h.

The limits on the double beta decay of  $^{168}\text{Yb}$  to the ground and excited states of  $^{168}\text{Er}$  were set at the level of  $\lim T_{1/2} \sim 10^{14}\text{--}10^{18}$  yr. A possible resonant neutrinoless double-electron capture in  $^{168}\text{Yb}$  to the  $(2)^-$  1403.7 keV excited level of  $^{168}\text{Er}$  was restricted to  $\lim T_{1/2} = 1.9 \times 10^{18}$  yr. The utilization of ytterbium with natural isotopic composition, containing only  $\sim 0.1\%$  of  $^{168}\text{Yb}$ , and the passive source technique (only few % detection efficiency) considerably limited the sensitivity. In particular, the achieved sensitivity is a few orders of magnitude worse in comparison to  $\lim T_{1/2} \sim 10^{21}\text{--}10^{22}$  yr achieved in the most sensitive experiments looking for double beta processes with charge increase, namely double-electron capture, electron capture with positron emission, and double-positron decay (references for these experiments can be found in [8]). The half-life of the  $2\beta^-$  decay of  $^{176}\text{Yb}$  to the  $2^+$  88.3 keV excited level of  $^{176}\text{Hf}$  was restricted to  $T_{1/2}^{2\nu(0\nu)} \geq 4.5(4.3) \times 10^{16}$  yr. The sensitivity is slightly worse than that in the previous

experiment [25] due to the strong contamination of the  $\text{Yb}_2\text{O}_3$  sample with  $^{176}\text{Lu}$  on the level of  $\sim 0.4$  Bq/kg.

The present sensitivity to double beta decay of  $^{168}\text{Yb}$  and  $^{176}\text{Yb}$  can be significantly improved using isotopically enriched material and an active source technique. An Yb-loaded liquid scintillator (see e.g. [26]), or an Yb-containing crystal scintillator (e.g. Yb-doped YAG [40]), or a new scintillation material with Yb could be viable possibilities for the realization of a source-equal-detector double beta decay experiment.

A liquid-liquid extraction based method to reduce the contamination of the  $\text{Yb}_2\text{O}_3$  sample in potassium, radium and thorium by 3, 34 and 68 times, respectively, has been developed. These results could pave the way to the use of ytterbium in a large-scale experiment aiming at the investigation of neutrino oscillations and/or double beta decay [26, 27]. A rather high contamination of the  $\text{Yb}_2\text{O}_3$  sample by lutetium could be reduced by selection of materials with different mineral origin. For instance, we have observed an order of magnitude variation of the  $^{176}\text{Lu}$  activity ( $\sim 2$  mBq/kg and  $\sim 20$  mBq/kg) in two samples of gadolinium oxide from different suppliers. This is despite the fact that lower lutetium contamination was observed in the material of a lower purity grade. Furthermore, the samples of cerium, erbium and neodymium (elements chemically similar to ytterbium) utilized in the double beta decay experiments [41, 8, 42] are characterized by a much less  $^{176}\text{Lu}$  activity on the level of 0.3–4 mBq/kg. Therefore, one should organize screening of materials of different origin before final purification of samples for a low counting experiment. Further purification of ytterbium from lutetium could be achieved by using chromatographic separation [43, 44, 45]. Development of the chromatographic purification method is in progress.

## 5 ACKNOWLEDGEMENTS

The group from the Institute for Nuclear Research (Kyiv, Ukraine) was supported in part by the program of the National Academy of Sciences of Ukraine “Fundamental research on high-energy physics and nuclear physics (international cooperation)”. O.G.P. was supported in part by the project “Investigations of rare nuclear processes” of the program of the National Academy of Sciences of Ukraine “Laboratory of young scientists”.

## References

- [1] V.I. Tretyak, Yu.G. Zdesenko, Tables of double  $\beta$  decay data – an update, *At. Data Nucl. Data Tables* 80 (2002) 83.
- [2] A.S. Barabash, Average and recommended half-life values for two-neutrino double beta decay, *Nucl. Phys. A* 52 (2015) 935.
- [3] M. Tanabashi et al. (Particle Data Group), *Phys. Rev. D* 98 (2018) 030001.
- [4] J.D. Vergados, H. Ejiri, F. Simkovic, Neutrinoless double beta decay and neutrino mass, *Int. J. Mod. Phys. E* 25 (2016) 1630007.
- [5] S. Dell’Oro, S. Marcocci, M. Viel, F. Vissani, Neutrinoless Double Beta Decay: 2015 Review, *AHEP* 2016 (2016) 2162659.
- [6] S.M. Bilenky, C. Giunti, Neutrinoless double- $\beta$  decay: A probe of physics beyond the standard model, *Int. J. Mod. Phys. A* 30 (2015) 1530001.
- [7] S.S. Ratkevich et al., Comparative study of the double- $K$ -shell-vacancy production in single- and double-electron-capture decay, *Phys. Rev. C* 96 (2017) 065502.
- [8] P. Belli et al., First search for  $2\varepsilon$  and  $\varepsilon\beta^+$  decay of  $^{162}\text{Er}$  and new limit on  $2\beta^-$  decay of  $^{170}\text{Er}$  to the first excited level of  $^{170}\text{Yb}$ , *J. Phys. G: Nucl. Part. Phys.* 45 (2018) 095101.
- [9] J. Kotila and F. Iachello, Phase-space factors for double- $\beta$  decay, *Phys. Rev. C* 85 (2012) 034316.
- [10] J. Kotila and F. Iachello, Phase-space factors for  $\beta^+\beta^+$  decay and competing modes of double- $\beta$  decay, *Phys. Rev. C* 87 (2013) 024313.
- [11] M. Hirsch, K. Muto, T. Oda, H.V. Klapdor-Kleingrothaus, Nuclear structure calculation of  $\beta^+\beta^+$ ,  $\beta^+/\text{EC}$  and  $\text{EC}/\text{EC}$  decay matrix elements, *Z. Phys. A* 347 (1994) 151.
- [12] F.F. Deppisch, M. Hirsch, H.Päs, Neutrinoless double-beta decay and physics beyond the standard model, *J. Phys. G: Nucl. Part. Phys.* 39 (2012) 124007.

- [13] H.Päs, W. Rodejohann, Neutrinoless double beta decay, *New J. Phys.* 17 (2015) 115010.
- [14] R. Winter, Double  $K$  Capture and Single  $K$  Capture with Positron Emission, *Phys. Rev.* 100 (1955) 142.
- [15] M.B. Voloshin, G.V. Mitselmakher, R.A. Eramzhyan, Conversion of an atomic electron into a positron and double  $\beta^+$  decay, *JETP Lett.* 35 (1982) 656.
- [16] J. Bernabeu, A. De Rujula, C. Jarlskog, Neutrinoless double electron capture as a tool to measure the electron neutrino mass, *Nucl. Phys. B* 223 (1983) 15.
- [17] Z. Sujkowski, S. Wycech, Neutrinoless double electron capture: A tool to search for Majorana neutrinos, *Phys. Rev. C* 70 (2004) 052501(R).
- [18] J. Meija et al., Isotopic compositions of the elements 2013 (IUPAC Technical Report), *Pure Appl. Chem.* 88 (2016) 293.
- [19] S. Eliseev et al.,  $Q$  values for neutrinoless double-electron capture in  $^{96}\text{Ru}$ ,  $^{162}\text{Er}$ , and  $^{168}\text{Yb}$ , *Phys. Rev. C* 83 (2011) 038501.
- [20] M. Wang et al., The AME2016 atomic mass evaluation, (II). Tables, graphs and references, *Chin. Phys. C* 41 (2017) 030003.
- [21] C.M. Baglin, Nuclear Data Sheets for  $A = 168$ , *Nuclear Data Sheets* 111 (2010) 1807.
- [22] M.S. Basunia, Nuclear Data Sheets for  $A = 176$ , *Nuclear Data Sheets* 107 (2006) 791.
- [23] V.E. Ceron, J.G. Hirsch, Double electron capture in  $^{156}\text{Dy}$ ,  $^{162}\text{Er}$  and  $^{168}\text{Yb}$ , *Phys. Lett. B* 471 (1999) 1.
- [24] M.I. Krivoruchenko, F. Šimkovic, D. Frekers, A. Faessler, Resonance enhancement of neutrinoless double electron capture, *Nucl. Phys. A* 859 (2011) 140.
- [25] A.V. Derbin, A.I. Egorov, V.N. Muratova, S.V. Bakhlanov, New limits on half-lives of  $^{154}\text{Sm}$ ,  $^{160}\text{Gd}$ ,  $^{170}\text{Er}$ , and  $^{176}\text{Yb}$  with respect to double  $\beta$  decay to the excited  $2^+$  states of daughter nuclei, *Phys. At. Nucl.* 59 (1996) 2037.

- [26] R.S. Raghavan, New Prospects for Real-Time Spectroscopy of Low Energy Electron Neutrinos from the Sun, *Phys. Rev. Lett.* 78 (1997) 3618.
- [27] K. Zuber, Double beta decay with large scale Yb-loaded scintillators, *Phys. Lett. B* 485 (2000) 23.
- [28] H. Park et al., Stable Isotope Production of  $^{168}\text{Yb}$  and  $^{176}\text{Yb}$  for Industrial and Medical Applications, *J. Nucl. Sci. Tech.* 45, suppl. 6 (2008) 111.
- [29] M. Laubenstein, Screening of materials with high purity germanium detectors at the Laboratori Nazionali del Gran Sasso, *Int. J. Mod. Phys. A* 32 (2017) 1743002.
- [30] S. Agostinelli et al., GEANT4—a simulation toolkit, *Nucl. Instrum. Meth. A* 506 (2003) 250.
- [31] M. Boswell et al., *IEEE-NS* 58(3) (2011) 1212; J. Allison et al., Geant4 developments and applications, *IEEE Trans. Nucl. Sci.* 53 (2006) 270.
- [32] O.A. Ponkratenko et al., Event generator DECAY4 for simulating double-beta processes and decays of radioactive nuclei, *Phys. At. Nucl.* 63 (2000) 1282.
- [33] V.I. Tretyak, private communication.
- [34] R.S. Boiko, Chemical purification of lanthanides for low-background experiments, *Int. J. Mod. Phys. A* 32 (2017) 1743005.
- [35] P. Belli et al., Search for double beta decay of  $^{136}\text{Ce}$  and  $^{138}\text{Ce}$  with HPGe gamma detector, *Nucl. Phys. A* 930 (2014) 195.
- [36] I. Kawrakow, D.W.O. Rogers, The EGSnrc code system: Monte Carlo simulation of electron and photon transport, NRCC Report PIRS-701, Ottawa, 2003.
- [37] G.J. Feldman, R.D. Cousins, Unified approach to the classical statistical analysis of small signals, *Phys. Rev. D* 57 (1998) 3873.
- [38] R.B. Firestone et al., *Table of Isotopes*, 8-th ed., John Wiley, New York, 1996 and CD update, 1998.

- [39] P. Belli et al., Search for double- $\beta$  decay processes in  $^{106}\text{Cd}$  with the help of a  $^{106}\text{CdWO}_4$  crystal scintillator, Phys. Rev. C 85 (2012) 044610.
- [40] P. Antonini et al., Properties of Yb:YAG scintillators, Nucl. Instrum. Meth. A 486 (2002) 220.
- [41] P. Belli et al., New limits on  $2\varepsilon$ ,  $\varepsilon\beta^+$  and  $2\beta^+$  decay of  $^{136}\text{Ce}$  and  $^{138}\text{Ce}$  with deeply purified cerium sample, Eur. Phys. J. A 53 (2017) 172.
- [42] A.S. Barabash et al., Double beta decay of  $^{150}\text{Nd}$  to the first excited  $0^+$  level of  $^{150}\text{Sm}$ : preliminary results, Nucl. Phys. At. Energy 19 (2018) 95.
- [43] M. Kumar, Recent trends in chromatographic procedures for separation and determination of rare-earth elements, A Review, Analyst 119 (1994) 2013.
- [44] M. Max-Hansen et al., Optimization of preparative chromatographic separation of multiple rare earth elements, J. Chromatogr. A 1218 (2011) 9155.
- [45] F. Ojala et al., Modelling and optimization of preparative chromatographic purification of europium. J. Chromatogr. A 1220 (2012) 21.